Original Investigation

Prediction of IDH Mutation Status in High-grade Gliomas Using DWI and High T1-weight DSC-MRI

Emetullah Cindil, MD, Halit Nahit Sendur, MD, Mahi Nur Cerit, MD, Nesrin Erdogan, MD, Filiz Celebi, MD, Nurullah Dag, MD, Emrah Celtikci, MD, Arda Inan, MD, Yusuf Oner, MD, Turgut Tali, MD

Rationale and Objectives: We aimed to evaluate the diagnostic performance of diffusion-weighted imaging (DWI) and dynamic susceptibility contrast-enhanced (DSC) magnetic resonance imaging (MRI) parameters in the noninvasive prediction of the isocitrate dehydrogenase (IDH) mutation status in high-grade gliomas (HGGs).

Materials and Methods: A total of 58 patients with histopathologically proved HGGs were included in this retrospective study. All patients underwent multiparametric MRI on 3-T, including DSC-MRI and DWI before surgery. The mean apparent diffusion coefficient (ADC), relative maximum cerebral blood volume (rCBV), and percentage signal recovery (PSR) of the tumor core were measured and compared depending on the IDH mutation status and tumor grade. The Mann-Whitney U test was used to detect statistically significant differences in parameters between IDH-mutant−type (IDH-m−type) and IDH-wild−type (IDH-w−type) HGGs. Receiver operating characteristic curve (ROC) analysis was performed to evaluate the diagnostic performance.

Results: The rCBV was significantly higher, and the PSR value was significantly lower in IDH-w−type tumors than in the IDH-m group ($p = 0.002$ and <0.001, respectively).The ADC value in IDH-w−type tumors was significantly lower compared with the one in IDH-m types ($p = 0.023$), but remarkable overlaps were found between the groups. The PSR showed the best diagnostic performance with an AUC of 0.938 and with an accuracy rate of 0.87 at the optimal cutoff value of 86.85. The combination of the PSR and the rCBV for the identification of the IDH mutation status increased the discrimination ability at the AUC level of 0.955. In terms of each tumor grade, the PSR and rCBV showed significant differences between the IDH-m and IDH-w groups ($p \leq 0.001$).

Conclusion: The rCBV and PSR from DSC-MRI may be feasible noninvasive imaging parameters for predicting the IDH mutation status in HGGs. The standardization of the imaging protocol is indispensable to the utility of DSC perfusion MRI in wider clinical usage.

Key Words: High-grade glioma; Isocitrate dehydrogenase mutation; Cerebral blood volume (CBV); Percentage signal recovery (PSR); Diffusion weighted imaging (DWI); Dynamic susceptibility contrast-enhanced MR imaging (DSC-MRI).

Abbreviations: **AA** anaplastic astrocytoma, **ADC** apparent diffusion coefficient, **AUC** area under the ROC curve, **DWI** diffusion-weighted imaging, **DSC** dynamic susceptibility contrast-enhanced, **GB** glioblastoma, **HGG** high-grade glioma, **ICC** intraclass correlation coefficient, **IDH** isocitrate dehydrogenase, **IQR** interquartile range, **rCBV** relative cerebral blood volume, **PSR** percentage signal recovery, **ROC** receiver operating characteristics, **WHO** World Health Organization

INTRODUCTION

High-grade gliomas (HGGs) are the most common primary malignant brain tumors in adults and have dramatic short survival rates (1). Several genetic and molecular biomarkers related to survival and treatment response have been identified within the past decade for characterizing gliomas genetically (2,3). Isocitrate dehydrogenase (IDH) is one of them and happens to be the most used parameter (4,5). Today, it is well known that IDH is related to cellularity and angiogenesis (6), and IDH-mutant−type (IDH-m−type) gliomas have better clinical outcomes than IDH-wild−type (IDH-w−type) forms do (3,4,5,7). IDH-m gliomas are also more responsive to temazolamide and radiotherapy (8,9). Therefore, IDH mutation is considered to be a prognostic biomarker in low-grade gliomas and HGGs (9,10).

Immunohistochemistry and genomic sequence analysis are the main methods used to detect IDH mutations in gliomas (6). However, these methods are studied from histopathological

Acad Radiol 2021; ■:1–11

From the Gazi University, School of Medicine, Department of Radiology, Ankara, Turkey (E.C., H.N.S., M.N.C., N.E., N.D., Y.O., T.T.); Yeditepe University, School of Medicine, Department of Radiology, Istanbul, Turkey (F.C.); Gazi University, School of Medicine, Department of Neurosurgery, Ankara, Turkey (E.C.); Gazi University, School of Medicine, Department of Pathology, Ankara, Turkey (A.I.). Received August 4, 2020; revised January 24, 2021; accepted February 3, 2021. **Address correspondence to:** E.C. e-mail: emetiyildirim@yahoo.com

https://doi.org/10.1016/j.acra.2021.02.002

samples that require invasive biopsy techniques. Also, a biopsy can lead to an incorrect result before surgical resection due to sampling errors or intratumoral heterogeneity. Therefore, a non-invasive, accurate method for predicting the IDH mutation status can have great potential in routine clinical practice.

Several conventional magnetic resonance imaging (MRI) features have been identified to detect the IDH mutation status in gliomas (11-16). IDH-m gliomas tend to appear in the frontal lobe (11-14) and have a relatively well-defined border (12) and a high apparent diffusion coefficient (ADC) value compared with IDH-w types (15,16). Some studies have also shown that IDH-m tumors have low vascular endothelial grow factor levels and show less contrast enhancement (12-14). Similarly, the area of necrosis was found to be larger in IDH-w−type tumors and may help in determining the IDH mutation status. However, these findings were not sufficient for accurately identifying the IDH mutation status.

Advanced MRI methods, such as diffusion-weighted imaging (DWI), have also been extensively studied to identify the IDH mutation status in HGGs (15-17). In particular, the ADC obtained through DWI provides important in vivo physiological information about the cellularity of brain tumors, and its use is increasing, including for tumor grading and molecular marker differentiation. Several studies have demonstrated lower ADC values in IDH-w−type HGGs than in IDH-m−type HGGs (15-17).

Dynamic susceptibility contrast-enhanced MRI (DSC-MRI) is the most prevalently used perfusion MRI technique. It is a non-invasive tool used for the initial diagnosis and evaluation of the treatment response of brain tumors. The technique is based on susceptibility variations during the first pass of a contrast agent bolus through the capillary bed. The relative cerebral blood volume (rCBV), the most commonly used parameter, reflects the microvascular density and angiogenesis. Several studies have also shown significant rCBV differences among HGGs according to the IDH mutation status in gliomas (6,11,17-19). This information suggests that tumor angiogenesis may differ according to the IDH genotype, and these differences may be distinguishable by DSC-MRI. The percentage of signal recovery (PSR) is another parameter of DSC-MRI and is obtained from the signal intensity time curve. PSR, as the name suggests, represents the percentage of signal intensity recovered relative to the baseline (signal intensity before contrast application) at the end of the first pass of the contrast agent. Following the application of the contrast agent, signal intensity decreases in the first step, and this is followed by recovery toward the baseline. This recovery rate, called PSR, provides information about blood-brain barrier integrity (BBB) and vascular permeability. In addition, it has been used to identify tumor characteristics, mostly in the initial differential diagnosis of HGGs, metastasis, and primary cranial nervous system lymphomas (20,21). To the best of our knowledge, no study has investigated PSR values obtained from DSC-MRI to determine the IDH mutation status in HGGs.

Although researchers in several studies have attempted to associate the genetic expression of a tumor with certain advanced MRI modalities, radiogenomic reports covering the genetic profiles in HGGs are not yet sufficient to implement in clinical practice in this area. The primary aim of this study was to noninvasively evaluate the diagnostic performance of perfusion and diffusion parameters in the discrimination of the IDH mutation status in HGGs.

METHODS

Study Design and Patient Selection

This retrospective study received approval from the institutional review board (REC number 2018/24074710-604.01.01-49), and informed consent was waived. Multiparametric MRI data, including the DWI and DSC perfusion weighted imaging (PWI) of 81 adult patients (older than 18 years) with histopathologically proved HGGs between January 2013 and February 2018, were derived and retrospectively analyzed. None of the patients received any brain tumor treatment at the time of imaging. An experienced neuropathologist histopathologically diagnosed all tumors on surgical resection specimens. The diagnosis was carried out according to the 2016 World Health Organization (WHO) classification criteria (22). Patients were excluded if the presence of IDH mutation was unavailable (n = 15) and if the image quality of DSC-MRI or DWI was insufficient due to artifacts or technical errors (n = 2). Five patients were diagnosed with oligodendroglioma (ODG) (Grade 2 ODG n=3, grade 3 ODG n= 2) and were excluded due to their low numbers. Consequently, 58 patients with 35 glioblastomas (GBs, 25 IDH-w types, 10 IDH-m types) and 27 anaplastic astrocytomas (AAs, 10 IDH-w types, 13 IDH-m types) formed the study population. Immunohistochemistry was performed to assess mutated IDH1 (R132H) protein expression. Genomic sequence analysis was performed for negative samples to identify non-canonical IDH1 or IDH2 genes (23). IDH mutation analysis was performed in all patients diagnosed with glial tumors as permitted by the technical facilities of the pathology department. No retrospective IDH mutation analysis was performed due to clinical or surgical suspicion. The mean interval between MRI and the operation was six days (range 0-12 days).

Imaging Acquisition

All MRI examinations were performed with a 3T scanner (Magnetom Verio; Siemens AG, Erlangen, Germany) using an 8-channel head matrix coil. The protocol for multiparametric MRI consisted of axial T1-weighted imaging (T_1WI), axial T2-weighted fast spin-echo imaging (T_2WI), axial T_2W FLAIR imaging, susceptibility-weighted imaging (SWI), DWI, DSC perfusion imaging, and post-contrast T1WI in three orthogonal planes, or 3D T_1WI, in the same order.

DWI was performed in the axial plane with a spin-echo echo-planar sequence with b-values of 0 and 1000 s/mm^2. The imaging parameters were as follows: TR = 15000 ms, TE = 90 ms,

section thickness = 3 mm with no gap, and FOV = 23 cm. ADC maps were generated automatically via the internal software.

DSC imaging was performed after the bolus injection of Gadobutrol (0.1 mmol/kg, a rate of 5 mL/s) (Gadovist, Bayer Health Care, Berlin, Germany) with a 10-second delay, and following a 20-mL saline flush by using a fast echo-planar T2-weighted gradient echo sequence. The imaging parameters were as follows: TR/TE = 1500/30 ms; flip angle (FA) = 90°; matrix = 128 × 128 mm; FOV = 23 cm; section thickness = 5 mm; and intersection gap = 1.5 mm. A total of 60 dynamic scans were performed with a temporal resolution of 1.38 s for each scan.

Image Processing and Analysis

All MRI data were transferred to an in-house software system, and two neuroradiologists (E.C., who had four years of experience in neuroradiology imaging, and Y.O., who had 16 years of experience in neuroradiology imaging) who were blinded to histopathological and molecular features, in consensus.

For ADC measurement, one to three small ROIs (0.2–0.4 cm^2) were placed manually on the darkest areas on the tumor core that corresponded to the enhancing area trying to avoid hemorrhagic, cystic, calcific areas, and macrovessels by the help of conventional MR sequences and SWI images, and the lowest value was taken into account.

CBV maps were automatically obtained by using a dedicated software program. The CBV measurement was performed using one to three small ROIs (0.6–0.8 cm^2) on the hot spots of the tumor areas on the CBV maps. Necrotic areas, vascular structures, and hemorrhagic and cystic regions were avoided with the help of superimposed FLAIR, SWI, and other conventional MR images. The CBV of the contralateral normal-appearing white matter (NAWM) was measured in the same way using ROIs of the same size. For the purpose of obtaining the rCBV, the values of the tumor core were divided into the values of NAWM, and the maximum rCBV values were recorded.

PSR was measured on the grayscale perfusion maps overlaid on contrast-enhanced T1W images of the tumor core with drawing small ROIs (0.6–0.8 cm^2) in the same manner as in the CBV measurement. PSR was acquired from the signal intensity time curve of the region of interest using the formula of (SIpost-SImin) / (SIpre-SImin). SIpre represents baseline signal intensity before the contrast arrival. SImin represents the signal intensity at the bottom point after the contrast arrival. SIpost reflects the level of signal recovery afterward. For all of the measurements, an attempt was made to exclude hemorrhagic, necrotic, and calcified regions using T2-weighted, T1-weighted, and SWI images.

For the evaluation of inter-reader agreement, the experienced radiologist repeated the measurement in the same manner two weeks later.

Statistical Analysis

All statistical analysis was performed using SPSS 23 (IBM, Chicago). All baseline quantitative data were described as the median with the interquartile range (IQR). The categorical variables were compared with the chi-square test or Fisher's exact test. Differences in the perfusion parameters and ADC values between IDH-m and IDH-w gliomas were assessed using the Mann-Whitney U test due to the non-normally distributed data. Receiver operating characteristic (ROC) curve analysis was used to evaluate the diagnostic performance of parameters in discriminating IDH-m gliomas from IDH-w gliomas. Also, a logistic regression analysis was calculated by combining parameters to determine their added value for predicting the IDH mutation status. Spearman's rank correlation coefficients were used to assess the relationship among perfusion metrics, ADC, and the IDH mutation status. Inter-session agreement was evaluated by using the intra-class correlation coefficient (ICC). $p < 0.05$ was considered to be statistically significant.

RESULTS

Patient Characteristics

The mean age did not differ between IDH-w−type (58 ± 14 years) and IDH-m−type (49 ± 17 years) gliomas ($p > 0.05$). IDH-w−type tumors (12 F, 23 M) tended to be seen in men, whereas IDH-m−type tumors (15 F, 8 M) tended to be seen in women ($p = 0.020$).

Perfusion Parameters

The detailed analysis results of perfusion metrics based on the IDH mutation status are summarized in Table 1. Figures 1 and 2 show representative cases of IDH-m−type and IDH-w−type tumors, respectively. The rCBV was significantly higher in the IDH-w−type HGGs than in the IDH-m HGGs (4.18 vs 2.49, respectively; $p = 0.002$, Table 1). ROC curve analysis revealed that the AUC value was 0.887 with a sensitivity of 0.86, a specificity of 0.83, and an accuracy of 0.86 at the optimal cutoff value of 3.00 in differentiation IDH-w−type HGGs from IDH-m−type HGGs (Table 2).

The PSR was significantly lower in the IDH-w−type HGGs than in the IDH-m−type HGGs (75.76 vs 99.12, respectively; $p \leq 0.001$, Table 1). The AUC value was 0.938 with a sensitivity of 0.91, a specificity of 0.83, and an accuracy of 0.87 at the optimal cutoff value of 86.85 in differentiation IDH-w−type HGGs from IDH-m−type HGGs (Table 2).

The ADC value was significantly lower in patients with IDH-w−type HGGs than those with IDH-m−type HGGs (0.862×10^{-3} mm^2/s vs 1.033×10^{-3} mm^2/s, respectively; $p = 0.023$, Table 1). The AUC value of the ADC (0.686) revealed lower diagnostic performance compared with the rCBV and PSR (Table 2).

Logistic regression analysis revealed that the combination of the rCBV and PSR increased the diagnostic ability at a significant level (AUC of 0.955). The addition of the ADC to these metrics did not improve the diagnostic performance. The results of univariate and multivariate logistic regression analysis are shown in Table 2, and information on the ROC curve analysis for HGGs is presented in Figure 3.

TABLE 1. Comparison of the Median Values of ADC From DWI, PSR and rCBV From DSC-MRI Between IDH-m and IDH-w Type Gliomas.

Parameters for all HGGs	IDH Mutant (n=23)	IDH Wild (n=35)	*p* Values[a]
rCBV	2.49 (2.22-3.01)	4.18 (3.26-5.71)	0.002
PSR	99.12 (92.80-107.90)	75.76 (69.70-82.66)	>0.001
ADC ($x10^{-3}$ mm^2/s)	1.033 (0.910-1.174	0.862 (0.759-1.071)	0.023[a]
Parameters for GBs (n=35)	IDH Mutant (n=10)	IDH Wild (n=25)	
rCBV	2.54(2.11-3.03)	4.19(3.20-6.88)	0.001
PSR	98.57 (86.91-109.09)	74.7 (69.92-83.43)	>0.001
ADC ($x10^{-3}$ mm^2/s)	1.067(0.955-1.208)	0.862(0.761-1.023)	0.019
Parameters for AAs (n=23)	IDH Mutant (n=13)	IDH Wild (n=10)	
rCBV	2.36(2.28-2.94)	4.14(3.58-5.27)	>0.001
PSR	99.12 (93.55-110.20)	77.56 (69.52-88.07)	<0.001
ADC ($x10^{-3}$ mm^2/s)	1.002(.837-1.174)	0.867(0.730-1.177)	0.438

HGG, high-grade glioma; GB, glioblastoma; AA, anaplastic astrocytoma; rCBV, relative cerebral blood volume; PSR, percentage signal recovery; ADC, apparent diffusion coefficient; DWI, diffusion weighted imaging; DSC-MRI, dynamic susceptibility contrast-enhanced MRI; IDH-m, isocitrate dehydrogenase mutant type; IDH-w, isocitrate dehydrogenase wild type

a *p* values were calculated by the Mann Whitney-*U* test.

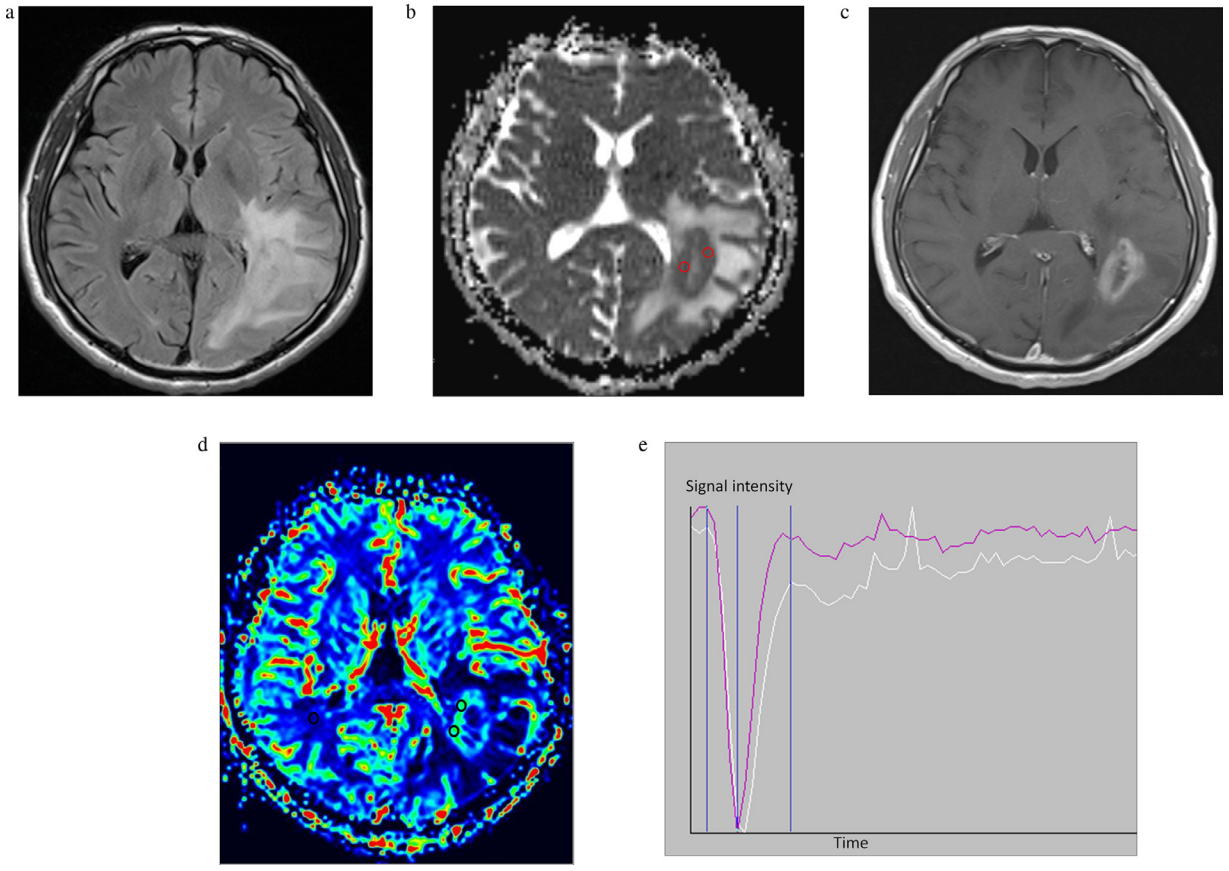

Figure 1. A 42-year-old woman with IDH-m−type glioblastoma at junction of left temporal-parietal and occipital lobes. Axial FLAIR image (a) demonstrates the large extension of peripheral edema. The measured ADC value was 0.976 × 10-3 mm2/s in the tumor core. Small red ROIs on the ADC map represent the ROI placement on the darkest areas of the tumor (b). Prominent peripheral contrast enhancement is seen on postcontrast axial T1WI (c). CBV slightly increased compared with the contralateral normal-appearing white matter, and rCBV was measured as 2.48 on CBV map (d). Small black ROIs represent the ROI placement on hot spots of the tumor and contralateral normal-appearing white matter (d). The signal intensity-time curve (e) returns close to the baseline, and PSR was measured 89.92.

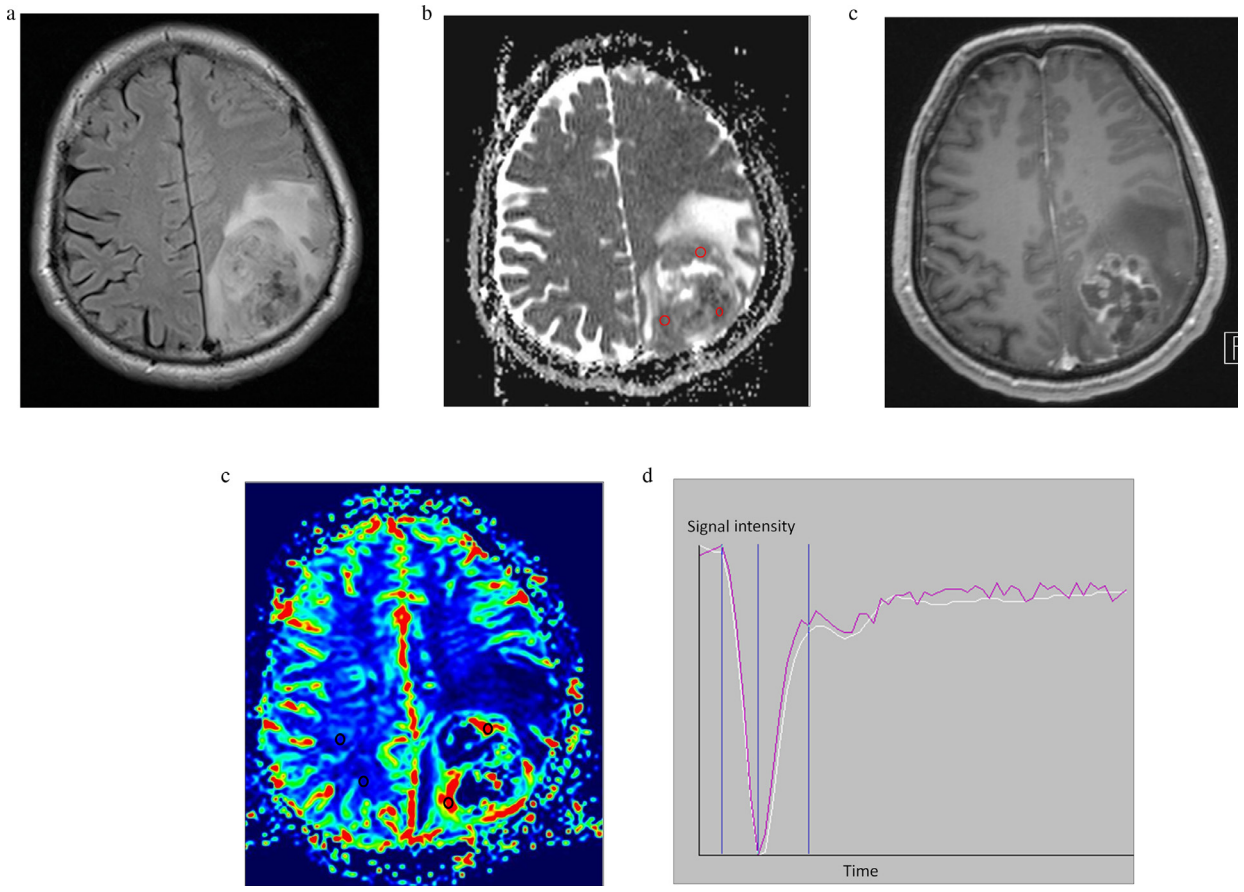

Figure 2. A 53-year-old man with IDH-w−type glioblastoma in left parietal lobe. FLAIR image (a) shows the extension of peripheral infiltrative edema. ADC value measured in tumor core is 0.942 × 10-3 mm2/s on ADC map (b). Small red ROIs on the ADC map represent the ROI placement on the darkest areas of the tumor (b). Postcontrast axial reformatted T1 MPRAGE (c) shows peripheral contrast enhancement. CBV map (d) reveals distinctive increased blood volume coded with red colors (Rcbv = 6.12). Small black ROIs represent the ROI placement on hot spots of the tumor and contralateral normal-appearing white matter (d).The signal intensity-time curve (e) shows partial return, and PSR was measured as 79.12.

TABLE 2. Diagnostic Performance of Each Parameter in Differentiation of IDH-mutant HGGs vs IDH-wild Type HGGs

Parameters for HGGs	AUC (95% CI) [a]	Cut-off	Sensitivity	Specificity	PPV/NPV	Accuracy
rCBV	0.887 (0.789-0.984)	3.00	0.86	0.83	0.88/0.83	0.86
ADC	0.686 (0.795-0.950)	0.954	0.74	0.66	0.77/0.58	0.68
PSR	0.938 (0.880-0.996)	86.85	0.91	0.83	0.87/0.85	0.87
CBV+PSR	0.955 (0.904-1.00)		0.95	0.94	0.92/0.97	0.95
Parameters for GBs						
rCBV	0.840 (0.660-1.00)	2.80	0.96	0.80	0.92/0.88	0.91
ADC	0.756 (0.573-0.939)	0.954	0.80	0.72	0.90/0.56	0.72
PSR	0.916 (0.824-1.00)	85.17	0.90	0.84	0.70/0.94	0.86
CBV+PSR	0.924 (0.838-1.00)		0.90	1.00	1.00/0.96	0.97
Parameters for AAs						
rCBV	0.962 (0.890-1.00)	3.26	0.90	0.92	0.82/0.92	0.87
PSR	0.938 (0.837-1.00)	92.20	0.92	0.80	0.86/0.89	0.90
CBV+PSR	1.00		1.00	1.00	1.00/1.00	1.00

HGG, high-grade glioma; AUC, area under the curve; CI, condifence interval; rCBV, relative cerebral blood volume; PSR, percentage signal recovery; GB, glioblastoma; AA, anaplastic astrocytoma; ADC, apparent diffusion coefficient; PPV, positive predictive value; NPV, negative predictive value.

a Univariate ve multivariate logistic regression analysis, and following ROC analysis were used to determine diagnostic performance.

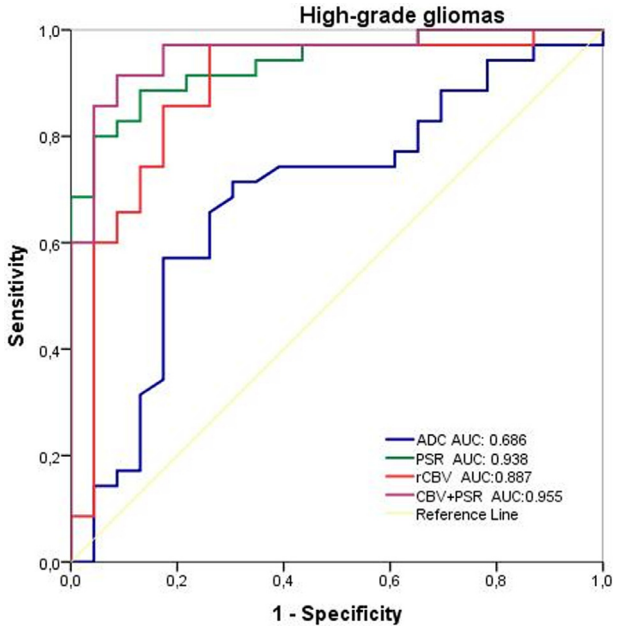

Figure 3. Receiver operating characteristic curves were presented in differentiation of IDH-wild−type high-grade gliomas from mutant types (for rCBV, PSR, ADC, and the combination of PSR and rCBV). The area under the ROC curve (AUC) was significantly higher for PSR, and the combination of PSR and rCBV improved the diagnostic performance.

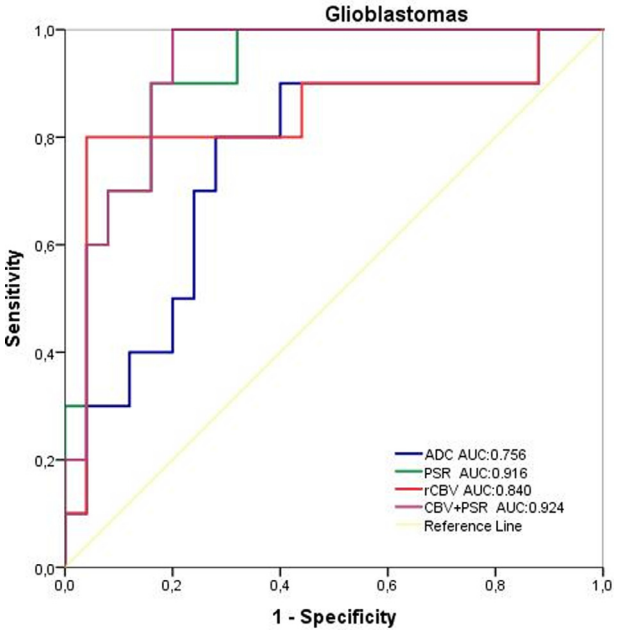

Figure 4. Receiver operating characteristic curves of glioblastomas to differentiate between IDH-wild and IDH-mutant-type lesions. PSR had superiority with AUC of 0.916, and the combination of PSR and CBV improved the diagnostic ability.

Finally, we used the same model approach to differentiate between IDH-m−type and IDH-w−type gliomas within each tumor grade. When the IDH mutation status was evaluated within GBs or AAs, wild-type tumors showed a significantly higher median rCBV value and a lower PSR value than mutant-type tumors did (4.19 vs 2.54 and 74.57 vs 98.57 for GBs; 4.14 vs 2.36 and 77.56 vs 99.12 for AAs, respectively; Tables 1 and 2). The AUC values were 0.840 for the rCBV and 0.916 for the PSR in GBs, and the AUC values were 0.962 for the rCBV and 0.938 for the PSR in AAs (Fig 4 and 5). For GBs, the mean ADC value in wild-type tumors was significantly lower than it was in mutant-type tumors (0.862 vs 1.067, respectively). For AAs, the mean ADC value showed significant overlaps between the mutant- and wild-type groups (1.002 vs 0.867, $p > 0.05$). The combination of the PSR and the rCBV in GBs improved the diagnostic ability with respect to the IDH mutation status (AUC = 0.924, Table 2). For AAs, the combination of the PSR and rCBV showed excellent discriminating performance regarding the IDH mutation status (AUC = 1.00, Table 2).

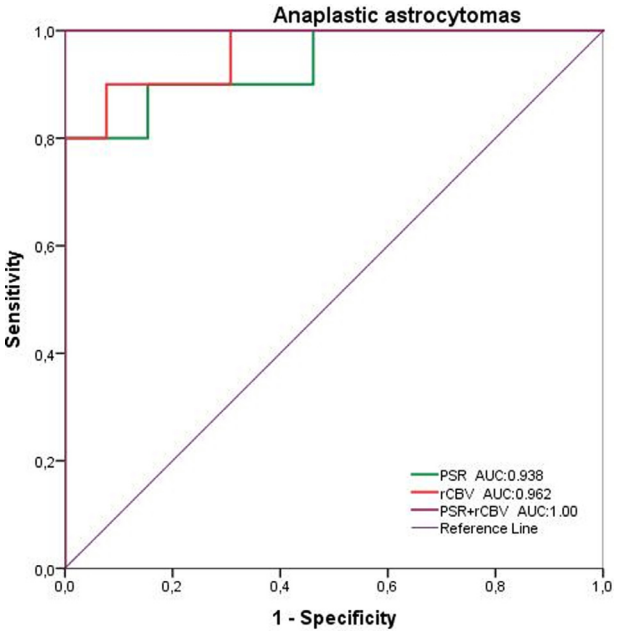

Figure 5. Receiver operating characteristic curves of anaplastic astrocytomas to differentiate between IDH-wild and IDH-mutant-type lesions. rCBV had the best diagnostic ability with AUC of 0.962, and the combination of PSR and rCBV yielded an excellent discrimination performance.

WHO Grade

When we evaluated the rCBV by the tumor grade, although GBs showed a higher median rCBV value than AAs did (3.56 (2.76-6.27) vs 2.97 (2.36-4.10), respectively; $p = 0.117$), the median values did not show a statistically significant difference. Similarly, other parameters (PSR and ADC) showed significant overlaps and did not differ between GBs and AAs ($p < 0.05$).

Correlation

The IDH mutation status showed a significant positive correlation with the rCBV ($r = 0.632$, $p < 0.001$) and a significant negative correlation with the PSR ($r = -0.656$, $p < 0.001$), as

well as a weak negative correlation with the ADC (r = -0.316, p = 0.016). The rCBV and PSR also showed a weak negative correlation (r = -0.389, p=0.001) with each other.

Repeatability

The intraclass correlation coefficient (ICC) was 0.898, 0.916, and 0.944 between two reading sessions for the rCBV, PSR, and ADC, respectively, which indicated excellent reproducibility.

DISCUSSION

The diagnostic values of the DSC-PWI and DWI parameters during the differentiation of the IDH mutation status in HGGs were evaluated in the present study. The results showed that besides having the highest correlation with the IDH mutation status (r = -0.656), the PSR also showed the best diagnostic performance with an AUC of 0.938 in determining the IDH mutation status in all parameters evaluated for HGGs. The rCBV was the second successful parameter with an AUC of 0.887 in HGGs, which was compatible with a few previous reports (6,11,18,19,24). The regression analysis revealed that the combination of the PSR and rCBV improved the diagnostic value of the determination of the IDH mutation status at a significant level for HGGs and also within each tumor grade.

ADC Analysis

The ADC in HGGs had a low diagnostic performance (AUC, 0.686) compared with the rCBV and PSR, and logistic regression analysis showed that the ADC did not make a significant impact on the discrimination of the IDH mutation status. On the other hand, when we evaluated tumor grades separately, the discrimination ability of the ADC increased at a significant level in GBs, which was consistent with previous studies (11). Lee et al. (16) reported an AUC value of 0.707 for the mean ADC in the discrimination of IDH-m−type and IDH-w−type HGGs (AAs and GBs), with significant overlaps found between tumor groups based on histogram analysis. Xing et al. (11) showed significantly lower ADC ratios in IDH-w GBs than in IDH-m GBs. In another study, Xing et al. (17) demonstrated that the minimum ADC and ADC ratio of IDH-m grade II-III astrocytomas were significantly higher than those of IDH-w−type ones with AUC values of 0.87 and 0.84, respectively. Similarly, Thust et al. (44 grade II/III gliomas) (25) and Villanueva-Meyer et al. (100 grade II gliomas) (26) reported statistically significantly lower ADC values for IDH-w−type tumors compared with IDH-m tumors. As a biomarker associated with tumor cellularity, the ADC value appears to be a useful adjunct in the differential diagnosis of the IDH mutation status of GBs only, not of AAs. A few studies also demonstrated that the rADC, the ratio of the value in the tumor core to the value in normal-appearing white matter, could also noninvasively detect IDH mutation in GBs (11,17,18,27). Interestingly, some studies suggested that the ADC is better for determining the IDH mutation status of gliomas compared with the rCBV (15-17,27). However, the presented diagnostic performance was still low in comparison with this study's PSR results. Further investigations of a larger population are warranted.

rCBV Analysis

The rCBV has been shown to be associated with tumor angiogenesis and microvessel density in HGGs, and the rCBV is a potential marker of tumor aggressiveness (28). It was also reported that HGGs with IDH mutation have lower levels of tumor angiogenesis, and they show low invasion and proliferation compared with wild-type tumors (6,13,19,24,29). Our data show that the rCBV is significantly associated with the IDH mutational status. IDH-w−type tumors had significantly higher rCBV values than IDH-m types did. Researchers in several studies have attempted to evaluate the diagnostic performance of the rCBV in predicting the IDH mutation status of gliomas (6,11,15-19,24,27), and a few of them have demonstrated findings similar to those of this study (17-19,24). For instance, Tan et al. (18) observed a higher rCBV ratio in IDH-w−type tumors compared with mutant types within each WHO grade of II, III, and IV astrocytomas with AUC values of 0.83, 0.86, and 0.94, respectively (sensitivity and specificity in the range of 0.82-1.00). However, some studies focused on determining the IDH mutation status showed significant overlaps in the rCBV ranges between groups (15,16,24). In addition, the studies mentioned above lacked the standardization of the cutoff values of perfusion metrics due to the variety of levels of the mean rCBV values of the groups (6,11,15-19,24,27). For instance, Xing et al. (11) similarly reported higher rCBV values in IDH-w GBs than in IDH-m GBs. However, the reported mean values (IDH-w= 8.93, IDH-m=5.08) were considerably higher than the values in the GBs of this study were.

Additionally, Hempel et al. (19) showed that the diagnostic performance of rCBV was significantly reduced by the inclusion of ODGs in the analysis of gliomas depending on the IDH mutation status. Some other studies (15,24) showed lower diagnostic performance, which may the result of populations with mixed ODGs and astrocytomas, similarly to Hempel et al. In contrast, Kickingereder et al. (6) revealed a higher mean rCBV histogram metric in IDH-w− type grade II, III, and IV glial tumors, including ODGs, compared with mutant types. The accuracy rate (88%) was so similar to that in this study. All ODGs have 1p/19q codeletion and IDH mutation. Due to high angiogenic activity, they may show higher microvascularity than astrocytomas do (30), and they have significant overlaps with GBs (31). It is obvious that differences in the patient selection group or in the inclusion of a small number of patients in studies may lead to discrepancies in diagnostic performance and mean rCBV levels.

Affects of Pre-load, Contrast Leakage Correction Methods and MRI Protocol on CBV

Differences in the selected sequence types (such as GRE-EPI or spin-echo EPI), image acquisition parameters, and post-processing leakage correction methods may also be the reason for the inconsistencies of studies when it comes to rCBV evaluation in the discrimination of the IDH mutation status (Table 3). Although the trend is to standardize the DSC-MR imaging protocol (32,33), the studies differed in terms of the aforementioned areas. When one decreases T1 weighting with low FAs (i.e., 35-60), a long time to echo and time to repeat may also permit the reduction of T1 contamination. However, these techniques can reduce the signal-to-noise ratio. The contrast leakage through a disrupted BBB in HGGs may cause undesired T1 contamination, which results in the underestimation or overestimation of the rCBV (34). For the purpose of minimizing these T1 effects and obtaining a more accurate CBV, some methods have been proposed, such as pre-load contrast agent dosing, post-processing leakage correction algorithms, and adapting to pulse sequence parameters (34,35). Each method has some limitations, and currently, no widely accepted and used T1 leakage correction method exist. On the other hand, the studies that used leakage correction methods (15,16) reported lower diagnostic performance for the rCBV in the differentiation of IDH-m−type from IDH-w−type gliomas compared with other studies. The findings of these studies (15,16) suggest that contrast leakage correction approaches to reduce undesired T1 dominancy may decrease the mean rCBV values, as well as the differences between the rCBV values of tumor types. The high T1-weighted MR protocol we used (high FA, low TE, no preload contrast, no correction method) demonstrated a good diagnostic performance for the rCBV in determining the IDH mutation status compared with the other studies mentioned above (15,16,24). Tan et al. (18) used an identical MRI protocol with this study and showed a diagnostic performance similar to that of this study (Table 3). Further efforts to utilize widely used standardized imaging sequences, contrast agents, and better algorithms are needed to minimize the T1 and T2 dominant extravasation effects, as well as to improve the imaging signal-to-noise ratio. This will increase the accuracy and repeatability of the parameters in glioma imaging.

PSR Analysis

The PSR obtained from the signal intensity time curve of DSC-MRI reflects BBB integrity and contrast leakage from tumor capillaries; thus it provides information about changes in capillary permeability (20). Previous studies revealed that BBB disruption and capillary permeability were higher in IDH-w−type tumors than in IDH-m gliomas (36). In connection with this, signal recovery after the signal drop on the time-signal intensity curve appears less in wild-type tumors probably due to the leaky and immature capillaries resulting

TABLE 3. Basic study design and imaging parameters of DSC-MRI of several studies from literature, which studied on IDH mutation status of gliomas.

Study (year) [reference]	No. of Patients (n)	WHO Grade	Magnet Strength (T)	Slice Thickness (mm)	Preload Gadolinium Based Contrast Agent	TR /TE (ms)	FA (degree)	Postproccesing Leakage Correction for CBV
Xing et al. (2019) [(11)]	75	IV	3	5	No	1000-1250/54	35	NP
Tan et al. (2017) [(18)]	86	II, III,IV	3	4	NP	1500/30	90	NP
Leu et al. (2017) [(15)]	65	II, III	1.5 and 3	4-6	Yes	1250-2000/23-35	35, 60, 90	Yes
Hong et al (2018) [(29)]	176	IV	1.5, 3	5 and 6	NP	1500-1600/29.3-30-40	35,60,90	No
Lee et al. (2015) [(16)]	52	III, IV	3	5	No	1500/30-40	35-90	Yes
Xing et al. (2017) [(17)]	42	II, III	3	5	No	1000-1250/54	35	NP
Hempel et al. (2019) [(19)]	100	II, III, IV	3	4	Yes	1130/31	NP	Yes
Choi et al. (2019) [(24)]	463	II, III, IV	1.5 and 3	5 and 6	NP	1550-1600/29.3-30-40	35-60-90	No
Kickengereder et al. (2015) [(6)]	73	II, III	3	5	Yes	2220/36	90	Yes

DSC-MRI, dynamic susceptibility contrast-enhanced MRI; TR, time-to-repeptition; TE, time- to- echo; FA, flip angle; NP, not provided; CBV, cerebral blood volume.

from increased neoangiogenesis (6,24,29). The use of the PSR in the differentiation of cranial tumors is not a new idea. Several studies have reported higher diagnostic performance for the PSR than for the rCBV in the differentiation of high-grade gliomas, metastasis, and primary cranial nervous system lymphomas (20,21). To our knowledge, no report exists on the PSR during the determination of the IDH mutation status in gliomas. Only Choi et al. (24) reported significantly high diagnostic accuracy when using a neural network model and when using raw signal intensity time curves from DSC-MRI for determining the IDH mutation status in grade II, III, and IV gliomas. They demonstrated that the signal recovery curve was less steep and attenuated in IDH-w−type gliomas than in IDH-m types, which reflects increased permeability in IDH-w−type tumors. They also revealed that the initial slope was steeper and larger in the signal intensity time curve in IDH-w−type gliomas than in IDH-m types, which indicates increased neoangiogenesis in IDH-w−type tumors (6,24,29). Similarly, the PSR values (signal recovery rates) in our cases with IDH-w−type tumors were significantly lower than those of the mutant types, indicating lower levels of the post bolus plateaus of the curves. In terms of the prediction analysis of the IDH mutation status, the PSR was the best discriminative parameter for this study. Unlike the rCBV, which requires leakage correction methods for accurate estimation, the PSR can easily be measured from raw data without the need for time-consuming correction algorithms and sophisticated software packages.

Affects of Pre-load, Contrast Leakage Correction Methods and MRI Protocol on PSR

On the other hand, such parameters as TE, FA, contrast dose, and field strength are also known to affect the PSR values measured by taking T1 and T2 * weight (37). Because the PSR is basically a parameter that depends on the contrast leakage effect, approaches that correct leakage effects (such as preload contrast administration, post-processing leakage correction methods, and adapting to pulse sequence parameters) to reduce T1 dominancy may decrease the variance in the PSR between tumor types. Thus, our T1-weighted acquisition protocol with no preload is probably the major cause of the high diagnostic performance of the PSR in HGGs. When it comes to distinguishing the IDH mutation status of gliomas, the PSR may provide more accurate results than the rCBV does by revealing the difference in capillary permeability. Although the PSR appears to be effective in differentiating the IDH mutation status in HGGs, we could not compare our data since there is no similar study in the literature. Conducting studies that involve more patients and that utilize a standardized MR protocol may provide us with more reliable information.

Combination of Parameters

Some earlier studies (13) reported highly promising results for conventional sequences of MRI in differentiating the IDH mutation status of gliomas. However, later studies revealed lower diagnostic performances for conventional sequences compared with DWI and DSC-MRI parameters (11,15,17). Xing et al. (17) and Leu et al. (15) suggested that the combination of the ADC, the rCBV, and conventional MR images together may improve the discrimination ability in identifying the IDH mutation status of gliomas compared with each parameter evaluation alone. In this study, the combination of the PSR and the rCBV significantly improved the diagnostic ability of the IDH mutation status in HGGs and in separate WHO grades. The two parameters show different characteristics, and the diagnostic performance observed in the regression analysis may be stem from these features. Although the PSR is a marker of capillary permeability, the rCBV reflects irregular immature neoangiogenesis. Consequently, findings of higher rCBV, lower PSR, and ADC values in wild-type tumors than in mutant types correspond to the higher levels of neoangiogenesis, capillary permeability, and cellularity in IDH-w−type HGGs, respectively.

Limitations

This study has some limitations. The inherent bias associated with retrospective analysis is the major limitation, so the results should be tested with a prospective study. Furthermore, the overall survival or progression-free survival could not be evaluated due to the retrospective nature of this study. In addition, ROI selection may have been subject to sampling bias due to excluding the cystic and necrotic areas with the help of conventional and other MRI sequences. However, ROI measurement results among different observers showed excellent agreement. Voxel-based calculations may provide more accurate results. The relationship between other molecular and genetic markers, as well as imaging findings could have also been evaluated. We focused only on the IDH gene mutation status to decrease the influencing factors. However, more studies should be done with multiple pieces of genetic information to investigate the effect of these markers on imaging properties. In addition, this study focused only on a relatively small patient population consisting of AAs and GBs, and excluding ODGs due to the low numbers of them. Given the high metabolic activity and angiogenesis observed even in grade II oligodendrogliomas, higher CBV values were found in ODGs than in astrocytomas (38). This property may decrease the variance in the rCBV between ODGs and other wild-type gliomas, but we could not predict if the PSR has discrimination ability in the differentiation of ODGs from IDH-m 1p/19q noncodeleted HGGs or IDH-w−type tumors. Further studies with larger populations that include ODGs are warranted to verify the results.

CONCLUSIONS

The results of our study demonstrate that DSC-MRI can serve as a noninvasive method for approximating the IDH mutation status in HGGs. The PSR that reflects capillary permeability shows higher leaky capillaries in IDH-w−type HGGs. Using the combination of the rCBV and PSR may be more useful for detecting the IDH mutation status, which provides valuable information on survival and treatment strategies.

COMPLIANCE WITH ETHICAL STANDARDS FUNDING

No funding was received for this study.

CONFLICT OF INTEREST

The authors declare that they have no confilict of interest.

ETHICAL APPROVAL

All procedures performed in studies involving human participants were in accordance with the ethical standards of the institutional and/or national research commitee and with the 1964 Helsinki Declaration and its later amendments or compareble ethical standards.

INFORMED CONCENT

As this is a retrospective study, formal consent is not required.

Name and Address of Instution Gazi University, Faculty of Medicine, 06500, Besevler, Ankara, Turkey

CONFLICT OF INTEREST

We declare that we have no conflicts of interest.

REFERENCES

1. Ostrom QT, Gittleman H, Liao P, et al. CBTRUS statistical report: primary brain and central nervous system tumors diagnosed in the United States in 2007-2011. Neuro Oncol 2014; 16(suppl 4):iv1–iv63. doi:10.1093/neuonc/nou223. Suppl 4.
2. Cancer Genome Atlas Research Network. Comprehensive genomic characterization defines human glioblastoma genes and core pathways [published correction appears in Nature. 2013 Feb 28;494(7438):506]. Nature 2008; 455(7216):1061–1068. doi:10.1038/nature07385.
3. Frattini V, Trifonov V, Chan JM, et al. The integrated landscape of driver genomic alterations in glioblastoma. Nat Genet 2013; 45(10):1141–1149. doi:10.1038/ng.2734.
4. Louis DN, Perry A, Reifenberger G, et al. The 2016 World Health Organization Classification of Tumors of the Central Nervous System: a summary. Acta Neuropathol 2016; 131:803–820.
5. Szopa W, Burley TA, Kramer-Marek G, et al. Diagnosticand therapeutic biomarkers in glioblastoma: current status and future perspectives. BioMed Res Int 2017; 2017:8013575doi:10.1155/2017/8013575.
6. Kickingereder P, Sahm F, Radbruch A, et al. IDH mutation status is associated with a distinct hypoxia/angiogenesis transcriptome signature which is non-invasively predictable with rCBV imaging in human glioma. Sci Rep 2015; 5:16238.
7. Hartmann C, Hentschel B, Wick W, et al. Patients with IDH1 wild type anaplastic astrocytomas exhibit worse prognosis than IDH1-mutated glioblastomas, and IDH1 mutation status accounts for the unfavorable prognostic effect of higher age: implications for classification of gliomas. Acta Neuropathol 2010; 120:707–718.
8. Miller JJ, Shih HA, Andronesi OC, et al. Isocitrate dehydrogenase-mutant glioma: Evolving clinical and therapeutic implications. Cancer 2017; 123 (23):4535–4546. doi:10.1002/cncr.31039.
9. SongTao Q, Lei Y, Si G, et al. IDH mutations predict longer survival and response to temozolomide in secondary glioblastoma. CancerScience 2012; 103(2):269–273.
10. Sanson M, Marie Y, Paris S, et al. Isocitrate dehydrogenase 1 codon 132 mutation is an important prognostic biomarker in gliomas. J Clin Oncol 2009; 27:4150–4154.
11. Xing Z, Zhang H, She D, et al. IDH genotypes differentiation in glioblastomas using DWI and DSC-PWI in the enhancing and peri-enhancing region. Acta Radiol 2019; 60(12):1663–1672. doi:10.1177/0284185119842288.
12. Qi S, Yu L, Li H, et al. Isocitrate dehydrogenase mutation is associated with tumor location and magnetic resonance imaging characteristics in astrocytic neoplasms. Oncol Lett 2014; 7(6):1895–1902. doi:10.3892/ol.2014.2013.
13. Carrillo JA, Lai A, Nghiemphu PL, et al. Relationship between tumor enhancement, edema, IDH1 mutational status, MGMT promoter methylation, and survival in glioblastoma. AJNR Am J Neuroradiol 2012; 33 (7):1349–1355. doi:10.3174/ajnr.A2950.
14. Lasocki A, Tsui A, Gaillard F, et al. Reliability of noncontrast-enhancing tumor as a biomarker of IDH1 mutation status in glioblastoma. J Clin Neurosci 2017; 39:170–175.
15. Leu K, Ott GA, Lai A, et al. Perfusion and diffusion MRI signatures in histologic and genetic subtypes of WHO grade II-III diffuse gliomas. J Neurooncol 2017; 134(1):177–188. doi:10.1007/s11060-017-2506-9.
16. Lee S, Choi SH, Ryoo I, et al. Evaluation of the microenvironmental heterogeneity in high-grade gliomas with IDH1/2 gene mutation using histogram analysis of diffusion-weighted imaging and dynamic-susceptibility contrast perfusion imaging. J Neurooncol 2015; 121(1):141–150. doi:10.1007/s11060-014-1614-z.
17. Xing Z, Yang X. Noninvasive assessment of IDH mutational status in World Health Organization grade II and III astrocytomas using DWI and DSC-PWI combined with conventional MR imaging. Am J Neuroradiol 2017; 38:1138–1144.
18. Tan W, Xiong J, Huang W, et al. Noninvasively detecting Isocitrate dehydrogenase 1 gene status in astrocytoma by dynamic susceptibility contrast MRI. J Magn Reson Imaging 2017; 45(2):492–499. doi:10.1002/jmri.25358.
19. Hempel JM, Schittenhelm J, Klose U, et al. In Vivo Molecular Profiling of Human Glioma: Cross-Sectional Observational Study Using Dynamic Susceptibility Contrast Magnetic Resonance Perfusion Imaging. Clin Neuroradiol 2019; 29(3):479–491. doi:10.1007/s00062-018-0676-2.
20. Mangla R, Kolar B, Zhu T, et al. Percentage of signal recovery derived from MR dynamic susceptibility contrast imaging is useful to differentiate common enhancing malignant lesions of the brain. Am J Neuroradiol 2011; 32. doi:10.3174/ajnr.A2441. 1004±1010https://doi.org/PMID: 21511863.
21. Nakajima S, Okada T, Yamamoto A, et al. Differentiation between primary central nervous system lymphoma and glioblastoma: a comparative study of parameters derived from dynamic susceptibility contrast-enhanced perfusion-weighted MRI. Clin Radiol 2015; 70(12):1393–1399. doi:10.1016/j.crad.2015.08.004.
22. Myung JK, Cho HJ, Park CK, et al. IDH1 mutation of gliomas with long-term survival analysis. Oncol Rep 2012; 28:1639–1644.
23. Tabouret E, Nguyen AT, Dehais C, et al. Prognostic impact of the 2016 WHO classification of diffuse gliomas in the French POLA cohort. Acta Neuropathol 2016; 132(4):625–634. doi:10.1007/s00401-016-1611-8.
24. Choi KS, Choi SH, Jeong B. Prediction of IDH genotype in gliomas with dynamic susceptibility contrast perfusion MR imaging using an explainable recurrent neural network [published online ahead of print, 2019 May 24]. Neuro Oncol 2019: noz095. doi:10.1093/neuonc/noz095.
25. Thust SC, Hassanein S, Bisdas S, Rees JH, Hyare H, Maynard JA, Brandner S, Tur C, Jäger HR, Yousry TA, Mancini L. Apparent diffusion coefficient for molecular subtyping of non-gadolinium-enhancing WHO grade II/III glioma: volumetric segmentation versus two-dimensional region of interest analysis. Eur Radiol 2018 Sep; 28(9):3779–3788. doi:10.1007/s00330-018-5351-0. Epub 2018 Mar 23. PMID: 29572636; PMCID: PMC6096613.
26. Villanueva-Meyer JE, Wood MD, Choi BS, Mabray MC, Butowski NA, Tihan T, Cha S. MRI Features and IDH Mutational Status of Grade II Diffuse Gliomas: Impact on Diagnosis and Prognosis. AJR Am J Roentgenol 2018 Mar; 210(3):621–628. doi:10.2214/AJR.17.18457. Epub 2017 Dec 20. PMID: 29261348; PMCID: PMC5823758.
27. Hong EK, Choi SH, Shin DJ, et al. Radiogenomics correlation between MR imaging features and major genetic profiles in glioblastoma. Eur Radiol 2018; 28:4350–4361.
28. Law M, Yang S, Babb JS, et al. Comparison of cerebral blood volume and vascular permeability from dynamic susceptibility contrast-enhanced perfusion MR imaging with glioma grade. AJNR Am J Neuroradiol 2004; 25(5):746–755.
29. Zhang L, He L, Lugano R, et al. IDH mutation status is associated with distinct vascular gene expression signatures in lower-grade gliomas. Neuro Oncol 2018; 20(11):1505–1516.

30. Latysheva A, Emblem KE, Brandal P, et al. Dynamic susceptibility contrast and diffusion MR imaging identify oligodendroglioma as defined by the 2016 WHO classification for brain tumors: histogram analysis approach. Neuroradiology 2019; 61(5):545–555. doi:10.1007/s00234-019-02173-5.
31. Lev MH, Ozsunar Y, Henson JW, et al. Glial tumor grading and outcome prediction using dynamic spin-echo MR susceptibility mapping compared with conventional contrast-enhanced MR: confounding effect of elevated rCBV of oligodendrogliomas corrected. AJNR Am J Neuroradiol 2004; 25:214–221.
32. Welker K, Boxerman J, Kalnin A, et al. ASFNRrecommendations for clinical performance of MR dynamic susceptibility contrast perfusion imaging of the brain. AJNR Am J Neuroradiol 2015; 36(6):E41–E51.
33. Ellingson BM, Bendszus M, Boxerman J, et al. Consensus recommendations for a standardized Brain Tumor Imaging Protocol in clinical trials. Neuro Oncol 2015; 17(9):1188–1198. doi:10.1093/neuonc/nov095.
34. Boxerman JL, Prah DE, Paulson ES, et al. The role of preload and leakage correction in gadoliniumbased cerebral blood volume estimation determined by comparison with MION as a criterion standard. AJNR Am J Neuroradiol 2012; 33(6):1081–1087.
35. Hu LS, Baxter LC, Pinnaduwage DS, et al. Optimized preload leakage-correction methods to improve the diagnostic accuracy of dynamic susceptibility-weighted contrast-enhanced perfusion MR imaging in post-treatment gliomas. AJNR Am J Neuroradiol 2010; 31(1):40–48.
36. Anzalone N, Castellano A, Cadioli M, et al. Brain gliomas: multicenter standardized assessment of dynamic contrast-enhanced and dynamic susceptibility contrast MR images. Radiology 2018; 287(3):933–943.
37. Boxerman JL, Schmainda KM, Weisskoff RM. Relative cerebral blood volume maps corrected for contrast agent extravasation significantly correlate with glioma tumor grade, whereas uncorrected maps do not. AJNR Am J Neuroradiol 2006; 27(4):859–867.
38. Saito T, Yamasaki F, Kajiwara Y, et al. Role of perfusion-weighted imaging at 3T in the histopathological differentiation between astrocytic and oligodendroglial tumors. Eur J Radiol 2012; 81:1863–1869.